AGU PUBLICATIONS

Water Resources Research

RESEARCH ARTICLE
10.1002/2017WR020871

Key Points:
- Nonlinear filtering effects of reservoirs on FFCs analyzed
- Threshold behavior revealed in FFC changing with reservoir regulation capacity
- Underlying processes consistently identified using models with varying complexity

Correspondence to:
H.-Y. Li,
hongyi.li@montana.edu

Citation:
Wang, W., Li, H.-Y., Leung, L. R., Yigzaw, W., Zhao, J., Lu, H., . . . Blöschl, G. (2017). Nonlinear filtering effects of reservoirs on flood frequency curves at the regional scale. *Water Resources Research*, *53*, 8277–8292. https://doi.org/10.1002/2017WR020871

Received 2 APR 2017
Accepted 31 AUG 2017
Accepted article online 8 SEP 2017
Published online 15 OCT 2017

Nonlinear Filtering Effects of Reservoirs on Flood Frequency Curves at the Regional Scale

Wei Wang[1,2], Hong-Yi Li[2,3], L. Ruby Leung[2], Wondmagegn Yigzaw[3], Jianshi Zhao[4], Hui Lu[1,5], Zhiqun Deng[2], Yonas Demisie[6], and Günter Blöschl[7]

[1]Ministry of Education Key Laboratory for Earth System Modeling, and Department of Earth System Science, Tsinghua University, Beijing, China, [2]Pacific Northwest National Laboratory, Richland, WA, USA, [3]Department of Land Resources and Environmental Sciences & Institute on Ecosystems, Montana State University, Bozeman, MT, USA, [4]State Key Laboratory of Hydro-science and Engineering, Department of Hydraulic Engineering, Tsinghua University, Beijing, China, [5]Joint Center for Global Change Studies, Beijing, China, [6]Department of Civil and Environmental Engineering, Washington State University, Pullman, WA, USA, [7]Institute of Hydraulic Engineering and Water Resources Management, Vienna University of Technology, Wien, Vienna, Austria

Abstract Reservoir operations may alter the characteristics of Flood Frequency Curve (FFC) and challenge the basic assumption of stationarity used in flood frequency analysis. This paper presents a combined data-modeling analysis of reservoir as a nonlinear filter of runoff routing that alters the FFCs. A dimensionless Reservoir Impact Index (RII), defined as the total upstream reservoir storage capacity normalized by the annual streamflow volume, is used to quantify reservoir regulation effects. Analyses are performed for 388 river stations in the contiguous U.S. using the first two moments of the FFC, mean annual maximum flood (MAF) and coefficient of variations (CV), calculated for the pre and post-dam periods. It is found that MAF generally decreases with increasing RII but stabilizes when RII exceeds a threshold value, and CV increases with RII until a threshold value beyond which CV decreases with RII. Hence depending on the magnitude of RII, reservoir regulation acts as a filter to increase or reduce the nonlinearity of the natural runoff routing process and alters flood characteristics. The nonlinear relationships of MAF and CV with RII can be captured by three reservoir models with different levels of complexity, suggesting that they emerge from the basic flood control function of reservoirs. However, the threshold RII values in the nonlinear relationships depend on the more detailed reservoir operations and objectives that can only be captured by the more complex reservoir models. Our conceptual model may help improve flood-risk assessment and mitigation in regulated river systems at the regional scale.

1. Introduction

Flooding is one of the most common natural hazards causing significant socioeconomic and ecological damages around the world (Messner & Meyer, 2006). Flood frequency analysis is conventionally used to estimate the flood risk of a specific location (Guo et al., 2014; Khaliq et al., 2006), with the basic assumption of independence and stationarity of the flood records (Gilroy & McCuen, 2012). However, during the last few decades, floods have exhibited nonstationarity due to climate change, land use change, and hydraulic structures (Milly, 2007; Franks & Kuczera, 2002; Viglione et al., 2016). Probabilistic analyses using the stationarity assumption may lead to over or underestimation of design floods and the associated risks if these changes are not accounted for (López & Francés, 2013).

The flood frequency curve (FFC) provides a comprehensive description of a catchment's storm response (Robinson & Sivapalan, 1997). River floods are the result of complex nonlinear processes involving precipitation, land use and land cover characteristics, and the drainage network (Wright et al., 2014). Three process groups are typically involved in flood generation: precipitation (forcing), runoff generation and concentration, and river routing. These processes are affected by climate change (Merz et al., 2012) as a warming climate can change the precipitation, snowmelt, and thus hydrologic regimes (Leung et al., 2004; Trenberth, 2011). Urbanization and land use change can also influence the runoff characteristics and dramatically affect runoff generation and concentration (Niehoff et al., 2002), and in-stream channel engineering such as reservoir operations can change the flood wave propagation and superposition (Hall et al., 2014; Maheshwari

et al., 1995). Hence, each of these processes is functioning as a nonlinear filter that fundamentally changes the frequency and magnitude of extreme events, in a sequential order, from precipitation to surface and subsurface runoff to channel flow. While land cover, soils, and channels could be considered as natural filters of extreme events, land use, and reservoirs act as anthropogenic filters of flood events, e.g., through their flood-peak enhancing property and reducing function.

Previous studies of flood frequency mainly focused on the impacts of climate change and urbanization on floods. Yang et al. (2013) examined the impacts of urbanization and climate change on urban floods in the upper midwestern United States and found that both the annual flood peak magnitudes and the annual peak-over-threshold flood magnitudes have increased. However, another study using the peak-over-threshold method on observations from the Central US reported no significant change in the magnitude of floods although considerable increases were found in the frequency of occurrence (Mallakpour & Villarini, 2015). Archfield et al. (2016) found clear trends in flood peak magnitudes across the United Sates, but there was little geographical cohesion of the trends, and the correlation with large-scale climate indices was rather weak. Sivapalan et al. (2005) applied a derived flood frequency methodology to explore the effects of land use and climate change on the FFCs. They found that the relative phase shift between climate forcing and catchment state determined the magnitude and shape of the FFCs.

To date, only a few studies focused on the impact of reservoir regulation on the FFCs. Case studies comparing rivers before and after dam construction showed a reduction in flood magnitude (Assani et al., 2006; Batalla et al., 2004) and interannual variability (Batalla et al., 2004) during the postregulation period. Magilligan and Nislow (2005) reported significant impacts of dams on hydrologic characteristics, especially on the temporal variation of minimum and maximum flows. Trend analyses of long-term annual peak floods across the continental U.S. demonstrated that most basins are affected by reservoir networks and regulation (Villarini et al., 2009). Several other studies (Franks & Kuczera, 2002; Gilroy & McCuen, 2009) found a change in extreme floods when nonstationary was considered in the flood frequency analysis.

While some research has focused on the impacts of reservoirs on the flood regime at individual locations, the extent and mechanism of modification of the FFC at the regional scale has not been fully explored. A better understanding of how rainfall, runoff generation, and routing are affected by climate change and human activities (Hall et al., 2014) and the resulting impacts on the FFCs is important for improving predictions of future changes. Extending the analysis of Blöschl and Sivapalan (1997) on the flood coefficient of variation (CV) as a function of rainfall duration and catchment residence time, this study considers the effects of reservoir regulation. Moreover, regionalization has been extensively used to estimate flood frequencies in ungauged sites, but most of the previous studies focus on the pristine catchments (Guo et al., 2014; Rosbjerg et al., 2013). Our goal is to provide a process-based understanding of how reservoir regulation affects the shape of the FFC quantified by its mean and CV, by combining observation data analysis and simple conceptual modeling. We adopt a regional perspective to allow an assessment over numerous reservoirs and large regions rather than individual dams, with the hope that the understanding gained from this exercise will shed light on the flood regionalization over human-influenced areas. In what follows, the data and methodology are introduced in section 2 and the results are presented in section 3. The paper concludes with a brief discussion and summary of the conclusion in section 4.

2. Data and Methodology

2.1. Data

To analyze the net effects of reservoir regulation on the FFC, a comparison of the FFCs derived for pre and post-dam periods is needed. Selecting streamflow gauges with sufficient record length is important for adequate sampling of the pre and post-dam conditions. As multiple reservoirs constructed over an extended period may be present in the upstream drainage area of a gauge, we define the pre-dam period as the period that ends when the first reservoir construction begins, while the post-dam period begins after the last reservoir construction is completed. Reservoir information is first obtained from the Global Reservoirs and Dams database (GRanD) (Lehner et al., 2011) that includes mostly reservoirs with a storage capacity more than 0.1 km^3, as shown in Figure 1a. Most of these reservoirs are operated with multiple objectives, including flood control. Long-term daily discharge records are obtained from U.S. Geological Survey (USGS, http://waterdata.usgs.gov/nwis/sw). All USGS gauges are filtered in a stepwise procedure. First, the locations

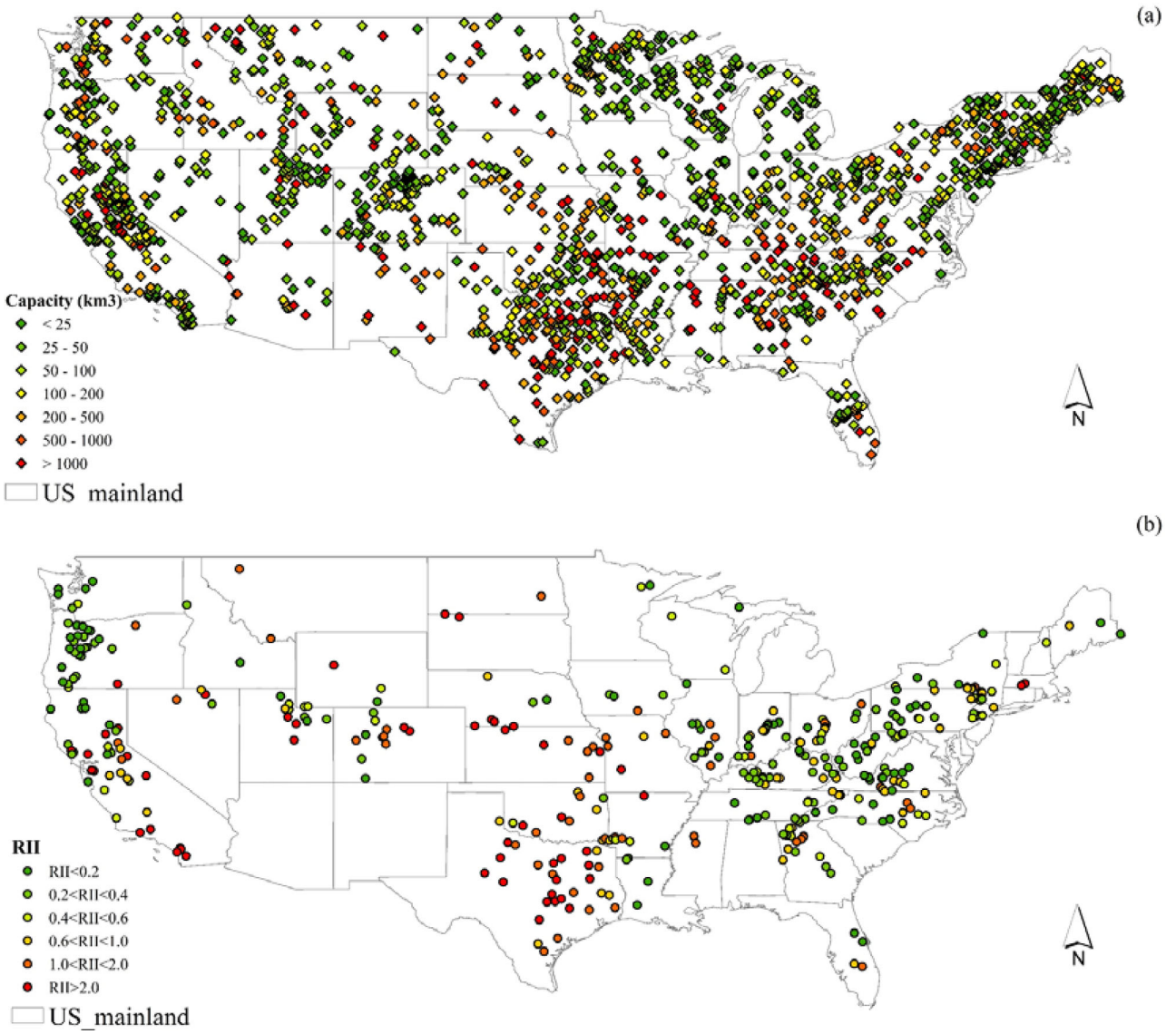

Figure 1. Spatial distribution of (a) 1887 dams from GRanD and (b) Reservoir Impact Index (RII) for the 388 stations used in the data analysis.

of all the GRanD reservoirs are overlaid on the upstream drainage area of each USGS gauge to determine all reservoirs that are located within the drainage area. Second, the USGS gauges with some reservoirs in their drainage areas are further filtered by the criterion of a minimum of 10 effective years with daily streamflow records in both the pre and post-dam periods. An effective year is defined as a year that contains daily streamflow records of more than 360 days. Third, to exclude the effects of landuse and climate change between the pre and post-dam periods, the gauges with significant change (20%) of annual mean streamflow values between pre and post-dam periods are excluded. Note that landuse and climate change may have impacts not only on the annual mean streamflow, but also on the seasonal cycle. Therefore, the third step does not exclude gauges that are subject to significant impacts of landuse and climate change on the seasonal water cycle, but little change in annual flow (e.g., warming causing earlier snowmelt). After filtering by the three-step procedure, 736 USGS gauges are selected.

The total reservoir storage capacity, defined as the summation of all reservoirs' storage capacity in the upstream drainage area of a USGS gauge, is a very important value to be used later in the analysis. Estimating this value from GRanD alone may lead to some bias by not including small reservoirs (with a storage capacity less than 0.1 km^3), since the GRanD database includes mostly larger reservoirs. In order to minimize

this type of bias, the Geospatial Attributes of Gages for Evaluating Streamflow, Phase II (GAGES-II) (Falcone, 2011) data set is used for reference, which includes dam and reservoir information for each gauge compiled from the National Inventory of Dams (NID). Note that GAGES-II does not provide exact dam construction time to derive pre and post-dam periods, so GAGES-II is used here mostly for referencing purposes. Besides, GAGES-II also supplements GRanD and provides an estimation of mean annual runoff for the period 1971–2000 considering the integrated effects of climate, land use, water use, and regulation. We compare the total reservoir capacity in the drainage area of each gauge calculated from GRanD and NID separately, namely S_{GRanD} and S_{NID}, and select those gauges with $|S_{GRanD} - S_{NID}|/S_{NID}$ less than 20%. After this procedure, the total number of selected USGS gauges is reduced to 388 for final analysis. As shown in Figure 1b, these 388 stations are spatially distributed quite evenly over the contiguous U.S. across various climatic and topographic conditions.

2.2. Statistical Moments of the Annual Maximum Flood

Based on the available data, annual maximum floods are derived from daily streamflow records and used to construct the FFC at each selected USGS gauge. To characterize the shape of the FFCs, the first two statistical moments of the distribution of annual maximum floods, i.e., the mean annual flood (MAF) and its coefficient of variation (CV), are estimated as:

$$MAF = \frac{1}{n}\sum_{i=1}^{n} x_i \tag{1}$$

$$CV = \frac{\sqrt{\frac{1}{n-1}\sum_{i=1}^{n}(x_i - MAF)^2}}{MAF} \tag{2}$$

where x_i is the observed annual maximum of daily streamflow in year i in m^3/s and n is the number of effective record years. In order to construct the FFCs, the annual maximum streamflow series are arranged and ranked in descending order. For the mth ranked peak flood, the exceedance probability and return period are then calculated as:

$$P(m) = \frac{m-a}{N+b} \tag{3}$$

$$T(m) = \frac{1}{P(m)} \tag{4}$$

where m is the mth ranked peak daily flood, $P(m)$ is the exceedance probability of the mth ranked data, $T(m)$ is the corresponding return period (years), N is the length of record, a and b are empirical parameters. In this paper, a and b are set to 0.44 and 0.12, respectively, following the recommendation by Gringorten (1963). The MAF and CV are calculated for all the gauges for the pre-dam and post-dam periods separately and compared to quantify the changes in the central tendency and variability of the FFCs due to reservoir regulation. The MAF captures the magnitude of floods while the CV represents the interannual variability. As the CV increases, the FFC curve becomes steeper and the floods are more variable.

MAF is usually a function of upstream drainage area of a gauge, i.e., the larger the area, the larger the MAF (Sivapalan et al., 1990). For the purpose of comparing the FFCs across different gauges, we use the dimensionless FFC to remove the impact of drainage area and hence, the magnitude of MAF. The dimensionless FFC is the FFC normalized by the MAF (i.e., the flood series are divided by MAF), so it is a dimensionless curve that captures only the flood interannual variability. Compared with the FFC, the corresponding dimensionless FFC has the same CV but with a mean value of 1. A three-parameter Generalized Extreme Value distribution (GEV) is fitted to the observed FFCs. The GEV is a common extreme value distribution that has been shown to well represent the maximum streamflow values in gauges over the contiguous U.S. (Vogel & Wilson, 1996). The cumulative distribution function of the GEV is:

$$F(x;\mu,\sigma,\xi) = \exp\left\{-\left[1+\xi\left(\frac{x-\mu}{\sigma}\right)\right]^{-1/\xi}\right\} \tag{5}$$

where μ is the location parameter, σ is the scale parameter, and ξ is the shape parameter. The return period of a given flood discharge is defined as:

$$T_{return} = \frac{1}{1 - F(x)} \tag{6}$$

The three parameters of the GEV are estimated by the maximum likelihood method for the pre-dam and post-dam records from which the expected normalized floods (flood discharge scaled by the mean annual flood) for different return periods (1.5, 2, 5, 10, 20, 50, 100 years) are calculated. For comparison, the Log-Pearson type III (LP3) distribution is also used to fit the flood series, but the results are very similar, so only the GEV-based results are shown in this paper.

2.3. Quantification of Reservoir Impact

To quantify the impact of reservoir regulation on flood peaks, a dimensionless Reservoir Impact Index (RII) is defined following López and Francés (2013):

$$RII = \frac{\sum_{j=1}^{m} S_j}{AMS \times T} \tag{7}$$

where S_j is the maximum storage capacity of reservoir j in the catchment area of the stream gauge, m is the total number of reservoirs in the catchment area of the gauge, AMS is the annual mean streamflow at the gauge, and T is the time of 1 year. Calculated as the total storage capacity of reservoirs in the catchment per unit volume of the annual streamflow, RII represents the degree of reservoir impacts within the 388 basins. Figure 1b shows the spatial distribution of RII estimated for the 388 gauges. The AMS values used in the RII calculation are obtained from the GAGES-II data set (Section 2.1).

2.4. Conceptual Models of Reservoir Regulation

In order to isolate the key processes during reservoir regulation, we develop three conceptual reservoir operation models with different levels of complexity but all accounting for flood control. First, a Simple Linear conceptual Model (SLM) is developed to facilitate process-based understanding of reservoir regulation impact on the FFC. The model represents reservoir operation of a flood-control reservoir at three stages (Figure 2): (1) when streamflow is lower than a threshold, the discharge is safe for the downstream reach, so there is no reservoir operation and the output discharge is the same as the input discharge; (2) when streamflow is above a threshold, the reservoir regulates the streamflow proportional to the input flood peak and the output discharge is smaller than the input; and (3) if the inflow exceeds the storage capacity of the reservoir, the reservoir no longer regulates the floods, and the output discharge is equal to the input discharge minus a discharge commensurate with the reservoir's maximum storage.

These three stages can be mathematically described as:

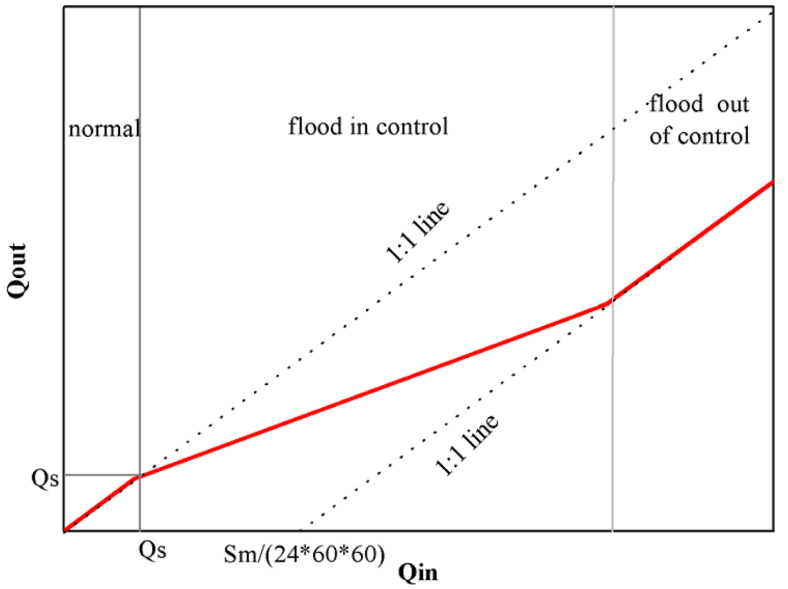

Figure 2. Operation rules (red line in the figure) for the Simple Linear concept Model (SLM) of equation (8).

$$Q_{out}=\begin{cases} Q_{in};\ Q_{in} < Q_s \\ 0.5*Q_{in}+0.5*Q_s;\ Q_s \le Q_{in} < 2*\dfrac{S_m}{24*60*60}+Q_s \\ Q_{in}-R;\ Q_{in} \ge 2*\dfrac{S_m}{24*60*60}+Q_s \end{cases} \quad (8)$$

where Q_s is the inflow threshold (m^3/s), Q_{in} is reservoir inflow (m^3/s, namely flood peak series), Q_{out} is regulated outflow (m^3/s), and S_m is the maximum storage capacity of the reservoir (m^3).

The model is only designed to capture the behavior of the annual maximum floods and the reservoir is assumed to be completely empty before flood-control operation begins. Such simplifications disregard the impact of initial storage on reservoir operation. For reservoirs with multiple purposes such as flood control and irrigation, the incoming streamflow is stored in the reservoir even if it is below the threshold until the reservoir is close to its full capacity, then the rule at stage 3 is used.

To explore how different aspects of reservoir regulation influence the FFC, we also adopt the Standard Operation Policy (SOP) hedging model (Morris & Fan, 1998) that includes the effects of both nonflood discharges and initial storage. The SOP conceptual model is further divided into two types: a simpler one, SOP1, where the water supply function of reservoirs is not accounted for; and a more complex one, SOP2, where the water supply function is represented as a function of water demand. In SOP1 a reservoir is represented using three parameters: maximum storage S_m, normal storage S_n, and flood limited storage S_c. The flood limited storage is the maximum reservoir water level that can be allowed before the flood season to preserve enough storage capacity for coming floods (Figure 3a). The following operation rules are invoked in SOP1 in the order of priority.

1. Water balance:

$$S(t+1)=S(t)+Q_{in}*\Delta t-Q_{out}*\Delta t \quad (9a)$$

2. For water storage in the reservoir:

$$0 \le S(t) \le S_m \quad (9b)$$

3. For regulated streamflow:

$$Q_e \le Q_{out} \le Q_s \quad (9c)$$

4. In the flood season: $S(t)$ should be less than S_c

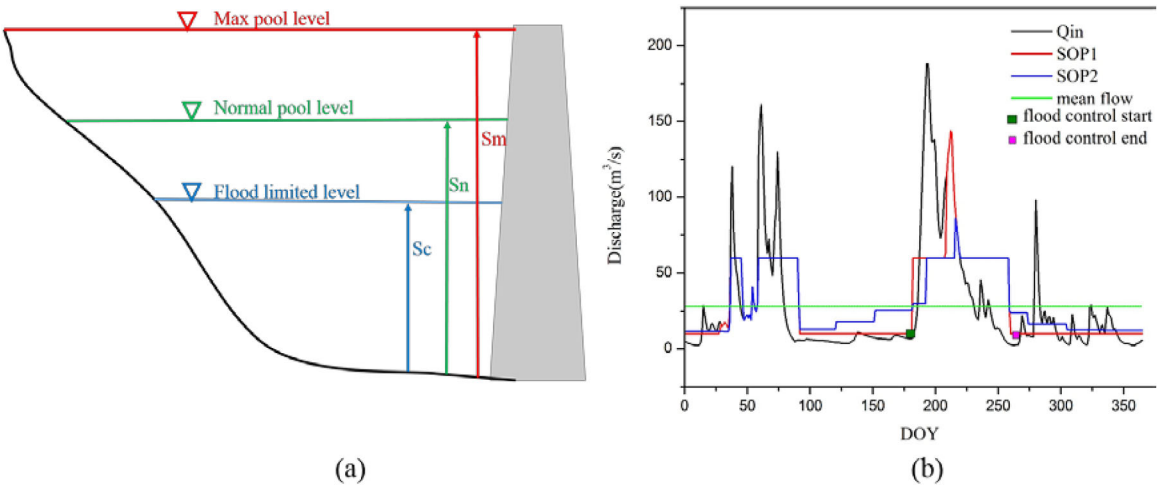

Figure 3. The Standard Operation Policy (SOP) hedging model (left) and discharge simulated by its variants, SOP1 (red) and SOP2 (blue), using observed inflow (black) as input to the models (right). The green line indicates the annual mean flow. The starting and ending dates of the flood control period are indicated by the green and magenta dots.

5. In the dry season: $S(t)$ should be kept at S_n

where, $S(t)$ is the water storage in the reservoir at time step t, Q_e is the environmental flow, Q_s is the maximum safe discharge for the downstream area, and Δt is the time step (1 day in this study).

The operations need to first satisfy Rule (1) then (2) and so on. If there are any conflicts between the rules, the rule with the higher priority is adopted and the other rules are abandoned.

Figure 3b shows an example of the results from SOP1 in one year of operation. In this example, S_m is set as $0.3*AMS*\mathrm{T}$ where T is taken as one year, and $S_n=0.7*S_m$, $S_c=0.3*S_m$, $Q_e=0.3*AMS$, $Q_s=2*$MAF. Here S_n and S_c are set using the average value from the reservoirs in the basin. Q_e is set to $0.3*AMS$ according to the Montana Method (Tennant, 1976), using the higher recommended value. Q_s is set according to the downstream flood control requirements. The SOP1 model is closer to the practical operation rules, especially for flood control reservoirs. This is because, for flood control reservoirs, SOP1 considers the discharge of the whole year and accounts for the reservoir initial storage. Thus, the water released by the reservoir is determined by the inflow and the remaining storage capacity at the beginning of the time step.

The regulated discharge in Figure 3b reflects the attenuation and filtering effects by the reservoir during the flood season. During spring, water storage in the reservoir is relatively low, and the reservoir has enough capacity to protect the downstream reaches against floods. During summer (DOY 150–250), two consecutive flood peaks occur. The first flood fills most of the reservoir storage, so the second flood cannot be mitigated by the reservoir because of the storage limit. Hence, the inflow during the second flood is largely discharged downstream. This implies that the peak of the regulated flow is determined by a combination of the previous storage and the inflow peak, a scenario not reflected by the SLM. As a result, the SOP1 operations are more realistic than the reservoir regulation process depicted in the SLM.

In SOP1, there is an assumption that during the nonflood season, the reservoir tends to store more water and release as little outflow as possible. For reservoirs that are operated for water supply in conjunction with flood control, this assumption may not be valid. In SOP2, the rules are modified during the nonflood season by replacing Rule (5) in SOP1. Thus, in SOP2, Rules (1)–(4) are the same as those in SOP1, followed by:

6. Q_{out} should be equal to Q_d if possible
7. In the dry season: $S(t)$ should be less than S_n if possible

Q_d is the water demand for the intended purposes, which varies during the year. For the same example discussed above, we set Q_d to vary within the year according to the monthly water usage in Sacramento, CA (http://projects.scpr.org/applications/monthly-water-use/city-of-sacramento/), while the mean value of Q_d is set as proportional to the annual discharge at the gauge (0.5 in this case). Other parameters such as S_n, S_m are kept the same as for SOP1. Figure 3b shows that the SOP2 release is larger than that of SOP1 during the nonflood season, which increases the reservoir storage space available for the flood season. Consequently, during the flood season, SOP2 produces smaller and more delayed flood peaks (after regulation) than SOP1. Generally, water supply (or other quantifiable demands such as electricity generation and irrigation) reservoirs can be better represented by SOP2 than by SOP1 and SLM.

3. Results and Discussion

In this section, we first present the observed emergent relationships between the flood frequency curve (FFC) and the Reservoir Impact Index (RII). The three conceptual models of different complexity are then used to identify and isolate the key reservoir regulation processes behind the observed patterns at the regional scale.

3.1. Emerging Patterns From Observations

Figure 4 shows scatter plots comparing the MAF and CV between the pre and post-dam periods. The post-dam MAF is smaller than the pre-dam MAF for most gauges, which is expected given the flood-peak-reducing function of reservoirs. On the other hand, the post-dam CV could be either larger or smaller than the pre-dam CV. Although on average, the post-dam CV slightly increases (from 0.598 to 0.632). Although this slightly higher CV is somewhat consistent with previous studies, e.g., (Assani et al., 2006), which offered an explanation that the normalized interyear variability increases after reservoir regulation, the mechanisms are much more complex so more analysis is warranted.

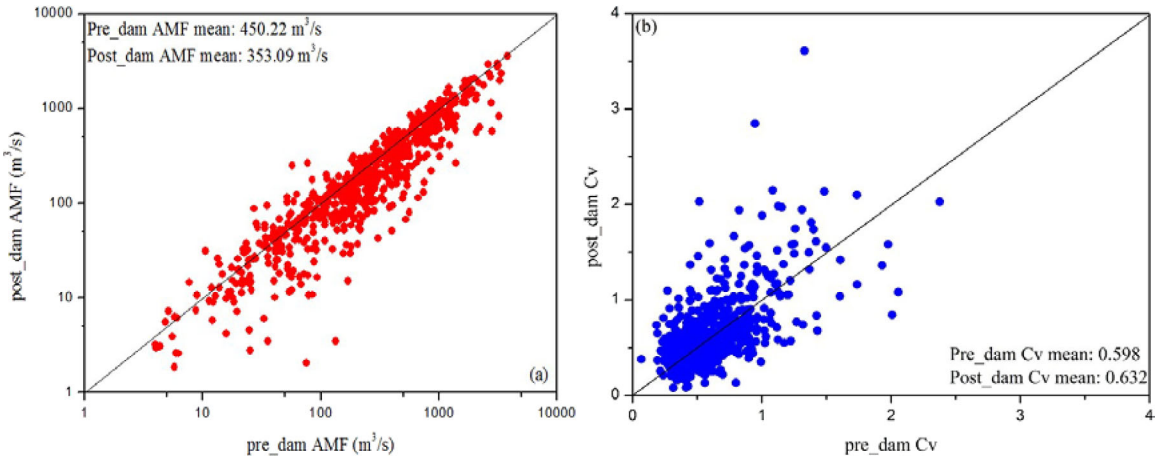

Figure 4. Scatter plots of (a) pre-dam mean annual flood (MAF) versus post-dam MAF and (b) pre-dam coefficient of variation (CV) versus post-dam CV. The mean values for the pre and post-dam periods are shown inside the boxes.

The absolute magnitude of the MAF largely reflects the site-specific characteristics such as the size of drainage area upstream. To eliminate the site-specific information embedded in the observational data as much as possible, Figure 5 plots the normalized MAF and CV in term of their relative changes against the corresponding RII values. The relative changes are defined as

$$\Delta MAF = \frac{\left(MAF_{post-dam} - MAF_{pre-dam}\right)}{MAF_{pre-dam}}$$

$$\Delta CV = \frac{\left(CV_{post-dam} - CV_{pre-dam}\right)}{CV_{pre-dam}} \tag{10}$$

To test the significance of the post-dam changes in the MAF, the nonparametric Mann-Whitney-Wilcoxon test (Mann & Whitney, 1947) is applied. As shown in Figure 5a, 246 out of the 388 gauges have experienced statistically significant post-dam MAF changes (significance level $\alpha = 0.05$). From the majority of the 246 gauges, ΔMAF generally becomes more negative as RII increases, then stabilizes at about -0.8 after RII reaches a threshold value (about 1.0). Theoretically, if the reservoir storage capacity is big enough to absorb all the incoming floods, water may be released at a constant discharge rate determined by the annual mean streamflow. In this case the relative change of MAF is

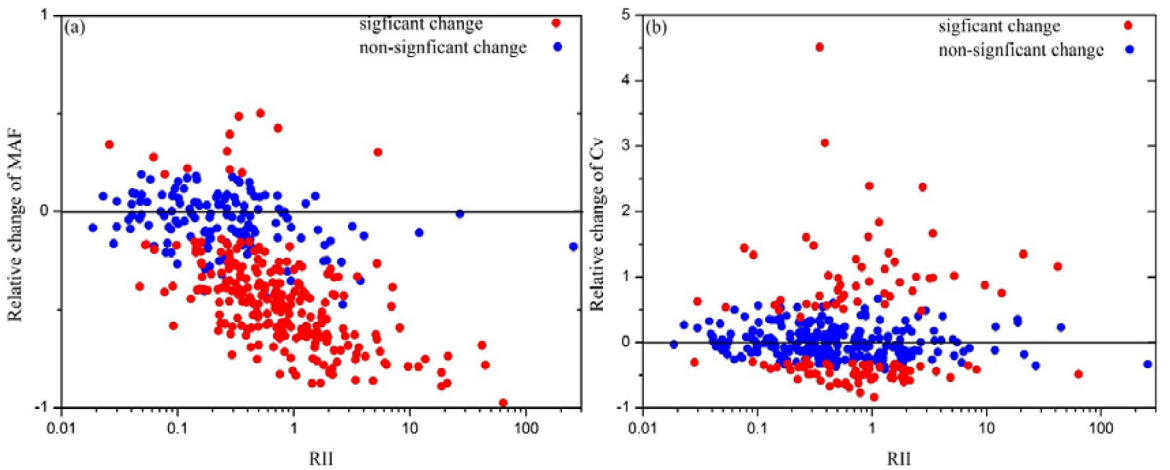

Figure 5. Relative changes of (a) mean annual flood (MAF) and (b) Coefficient of Variation (CV) between the pre-dam period and post-dam period as a function of the Reservoir Impact Index (RII). The horizon black lines are 0 lines. Gauges with significant and nonsignificant changes are indicated by red and blue dots, respectively.

$$\Delta MAF = \frac{\left(AMS - MAF_{pre-dam}\right)}{MAF_{pre-dam}} = \frac{AMS}{MAF_{pre-dam}} - 1 \quad (11)$$

Over the 388 gauges, the mean of $AMS/MAF_{pre-dam}$ is about 0.07, leading to $\Delta MAF \approx -0.93$. In reality, however, it is almost impossible for a reservoir to completely absorb all the incoming floods. Equation (11) provides an estimate of the upper limit of ΔMAF.

Among the 246 gauges, only 14 gauges have a significant increase in the MAF. Over these gauges, the reservoir regulation effects are likely dominated over by other factors. One possible reason for the increase is their relative position downstream of a reservoir. Twelve of the 14 gauge stations are found at a distant location from the reservoirs. The river segments between these stations and their upstream reservoirs are subject to larger lateral flow contribution, which itself could be subject to the effects of landuse change or surface water withdrawal. Another possible reason is that the climate conditions could have been altered by global warming that influence evaporation and increase interannual variability of extreme precipitation events. For such gauges, the effects of reservoir regulation might have been masked by the changes in lateral flow and/or climate change.

The significance test for the CV change is based on the method outlined in Miller (Edward Miller, 1991), with a focus on the CV of the dimensionless FFC. Note that the CV of the FFC is the same as the standard deviation of the dimensionless FFC. Hence conducting a test on the variance of the dimensionless FFC is equivalent to performing a test on the CV of the original FFC. The Levene's test (Gastwirth et al., 2009) is adapted to test the significance of the CV change after regulation. For the dimensionless FFC, its CV is equal to its standard deviation (STD), since the mean value of the dimensionless FFC is 1. Thus the test of FFC CV change can be transferred to test the STD change of the dimensionless FFC (Edward Miller, 1991). Only 123 gauges have experienced statistically significant post-dam CV change at $\alpha = 0.05$ level (see the red dots in Figure 5b). As RII increases, the 123 gauges branch off with some gauges showing positive ΔCV (higher post-dam period CV values) and others showing negative ΔCV (lower post-dam CV values). The positive and negative ΔCV values in Figure 5b roughly show a symmetric pattern, i.e., the absolute value of ΔCV increases with RII first, then it decreases, again interestingly, at a RII threshold of about 1.0.

Based on the patterns in Figures 4 and 5, a few questions warrant further investigation: (1) Why does ΔMAF decrease systematically with RII and then stabilize above a threshold value (i.e., RII $\approx$ 1.0)? (2) What causes the positive and negative changes of the CV during the post-dam period? (3) Is there any threshold behavior in the $\Delta CV \sim RII$ relationship (namely how ΔCV changes with RII) and why? These questions are addressed in the following subsection using the conceptual models introduced in Section 2.

3.2. Process Understanding Using Conceptual Models

One of the 388 USGS gauges, USGS ID 03574500 (Paint Rock River near Woodville AL), is arbitrarily chosen to illustrate whether and how well the three conceptual models reproduce the patterns of the MAF and CV changes in Figure 5. This gauge has a drainage area of 813.8 km^2, and a total storage of 2.36×10^5 m^3 from two dams, and an RII value of 0.0004 according to NID. The observed time series of floods are used as inputs to SLM, and the time series of daily streamflow is used as an input to SOP1 and SOP2. Here we prescribe the reservoir parameters to vary continuously to mimic different reservoir systems. For example, the reservoir storage capacity R is varied to represent RII values ranging from 0 to 10. As shown in Figure 6, varying RII continuously produces the curves of ΔMAF and ΔCV, and the different dots in the curves correspond to reservoir systems with different storage capacities.

Despite the different levels of complexity, all three models produce similar patterns: (1) ΔMAF becomes more negative as RII increases and then it stabilizes at about $-0.7 \sim -0.8$ after RII reaches a threshold value, similar to the pattern shown in Figure 5a; (2) As RII approaches the same threshold value as in the ΔMAF curve, ΔCV first increases gradually to a peak value with a positive CV change and then it drops steeply to a negative CV change after RII exceeds the threshold value. With the increasing of RII, for any specific reservoir larger and larger incoming floods can be efficiently regulated, thus leading to more negative ΔMAF . On the other hand, when RII is not sufficiently large, the eliminating of smaller floods (while leaving much larger floods unregulated) may first increase the variance among the floods then decrease. When RII is large enough, all incoming floods are completely regulated by the reservoirs, i.e., MAF approaches MAS and $CV_{post-dam}$ approaches zero, so both ΔMAF and ΔCV reaches their theoretical limits according to

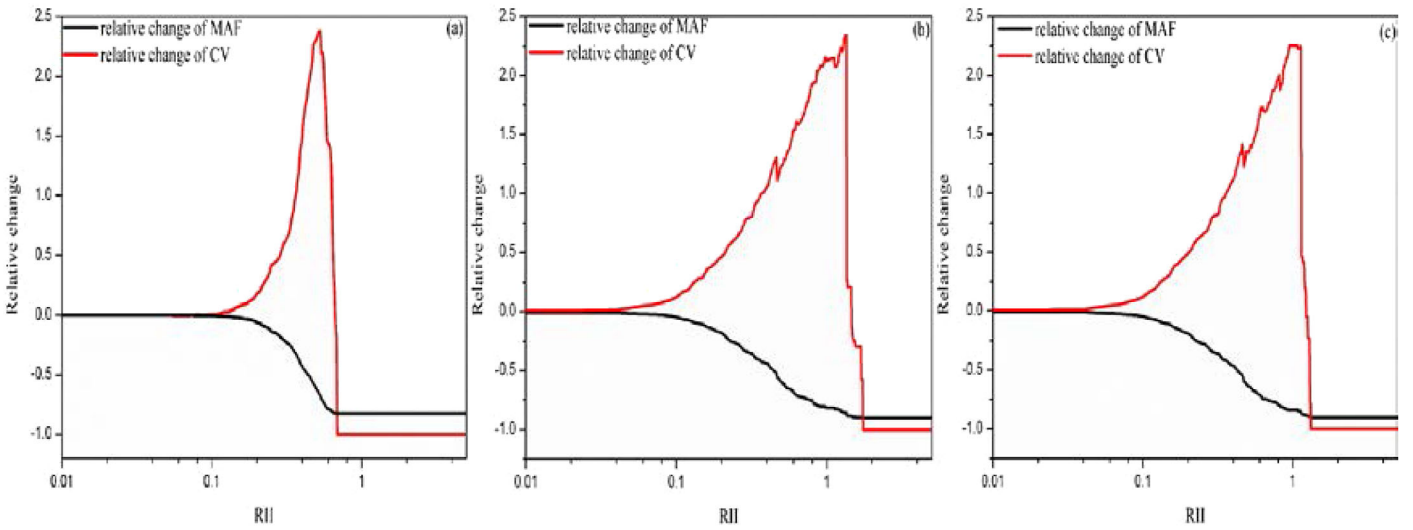

Figure 6. Simulations of the relative changes of the mean annual flood (MAF, black) and the coefficient of variation (CV, red) as a function of the Reservoir Impact Index (RII) using three conceptual models: (a) SLM, (b) SOP1, and (c) SOP2 (see equations (8)–(10)).

equations (10) and (11) for the SLM, SOP1, and SOP2 models. More discussion on the threshold behavior of MAF and CV of floods will be provided in the following analysis.

The use of SLM results in a lower threshold of RII where ΔCV reaches its peak value. This is because SLM only operates on flood peaks, without considering the effects of initial reservoir storage or flood duration. Such an assumption implies that the total reservoir storage capacity is available for dampening the incoming flood peaks, while in the case of SOP some initial reservoir storage has been occupied by nonflood streamflow, leaving less reservoir storage space for the incoming flood peaks. SOP1 results in a larger RII threshold value because the complete streamflow series are used as inputs and the model accounts for initial reservoir storage. With SOP2, the RII threshold value corresponding to the peak ΔCV is slightly smaller than that of SOP1. Note that the only difference between SOP2 and SOP1 is a water demand parameter in SOP2. In fact, SOP1 can be treated as a special case of SOP2 where Q_d equals to 0 in all the years. In SOP2, the reservoir releases more flow during the nonflood season to satisfy water demand, as shown in Figure 3b. As a result, the reservoir has more capacity to hold floods compared to SOP1. This extra storage leads to a larger flood-peak reduction in SOP2 than in SOP1.

Figure 7 and Table 1 show the FFCs and the dimensionless FFC for different RII values from the SOP2 simulations. When RII is smaller than the RII threshold value, reservoir regulation mainly reduces the small floods

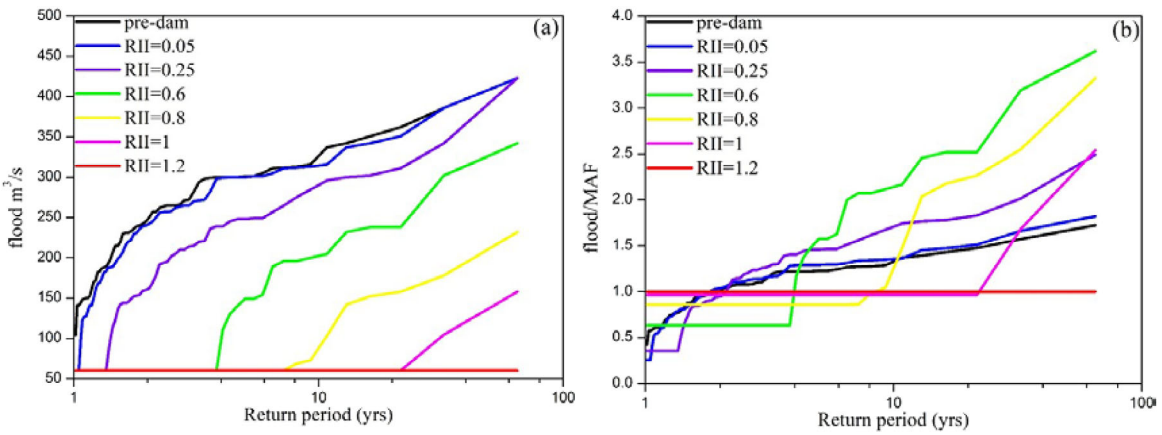

Figure 7. (a) FFCs and (b) dimensionless FFCs for different Reservoir Impact Indexes (RII) simulated by SOP2. Simulations are shown for the pre-dam condition (black) and for different RII values (different colors).

Table 1
Simulated Flood Results of the Standard Operation Policy (SOP2) Model for Different Values of the Reservoir Impact Index (RII)

	Flood/MAF						
Return period	pre_dam	RII = 0.05	RII = 0.25	RII = 0.6	RII = 0.8	RII = 1	RII = 1.2
1.24	0.74	0.72	0.35	0.63	0.86	0.96	1.00
2.02	1.02	1.04	0.95	0.63	0.86	0.96	1.00
5.00	1.23	1.29	1.46	1.58	0.86	0.96	1.00
9.37	1.29	1.35	1.68	2.12	1.05	0.96	1.00
22.38	1.47	1.51	1.83	2.52	2.26	0.96	1.00
34.28	1.57	1.66	2.01	3.19	2.55	1.68	1.00
73.23	1.72	1.82	2.49	3.62	3.32	2.54	1.00
	Flood (m^3/s)						
Return period	pre_dam	RII = 0.05	RII = 0.25	RII = 0.6	RII = 0.8	RII = 1	RII = 1.2
1.24	182	168	60	60	60	60	60
2.02	250	242	162	60	60	60	60
5.00	301	300	248	149	60	60	60
9.37	316	313	285	200	73	60	60
22.38	362	351	311	238	158	60	60
34.28	386	386	342	302	178	105	60
73.23	423	423	423	342	232	158	60

(hence reduced MAF), but the big floods are not affected much. Therefore, the dimensionless floods (floods normalized by the MAF) at large return periods (such as 50 or 100 years) may increase as a result of the reduced MAF, leading to a steeper post-dam dimensionless FFC (implying an increase in the post-dam CV). On the other hand, for RII greater than the threshold value, larger floods can also be regulated significantly. The rapid flattening of the dimensionless FFC beyond the RII threshold value in Figure 7 (corresponding to the rapid decrease of ΔCV in Figure 6) is in part due to the fact that the change of a large flood generally affects the CV of the FFC more significantly than the change of a small flood because of the positive skew of flood peak distributions. Figure 7 can be used to explain the threshold behavior shown in Figures 5 and 6. When RII is large enough, even bigger incoming floods are regulated by the reservoir(s) to the same level, i.e., a constant outflow from the reservoir(s). When RII is sufficiently large, all floods are fully regulated and the post-dam FFC loses completely its interannual variability (the red lines).

To check the reliability of the conceptual models, SOP2 is applied to the 123 gauges with significant changes in CV, i.e., those highlighted in red in Figure 5b. For these gauges, S_m, S_n and S_c are set according to the actual operating conditions. Q_m, Q_e, and Q_d are set to a fixed ratio of AMS at the gauge as $Q_m = 2 * AMS$, $Q_e = 0.3 * AMS$, and $Q_d = 0.5 * AMS$. The flood season is defined as the months (in a year) with mean discharges higher than *MAF* while the rest of the months are defined as the nonflood season. After SOP2 is set up for each gauge, the pre-dam period daily discharge records are used as inputs to SOP2 to simulate the regulated flood series. Figure 8 shows a comparison of the observed and SOP2 simulated ΔCV. We can see that in most gauges (93 out of 123 with statistically significant observed changes in CV), the SOP2 results are close to the observations. However, there are some gauges where the SOP2 simulated ΔCV values are in the opposite direction of the observed ΔCV values. For gauges with CV increases in the SOP2 simulation but decreases in observation, their RII values are usually less than 1.0. One likely reason of this inconsistency is the between-reservoir interactions within the upstream drainage area of a gauge, which is neither reflected in the definition of RII nor in the SOP2 model, as both assume independence between reservoirs. If several reservoirs exist in the same basin, the operation of one reservoir may well be dependent on the others. Hence a group of reservoirs may have more regulation power than the sum of the individual reservoirs. Another possible reason is that, in practical operations, the reservoir managers may consider future incoming streamflow series, for example based on hydrologic forecasts, to maximize the marginal benefits of reservoir operation. Such considerations are not included in SOP2. For gauges where the post-dam CV decreases in SOP2 but increases in the observations, their RII values are mostly larger than 2.0,

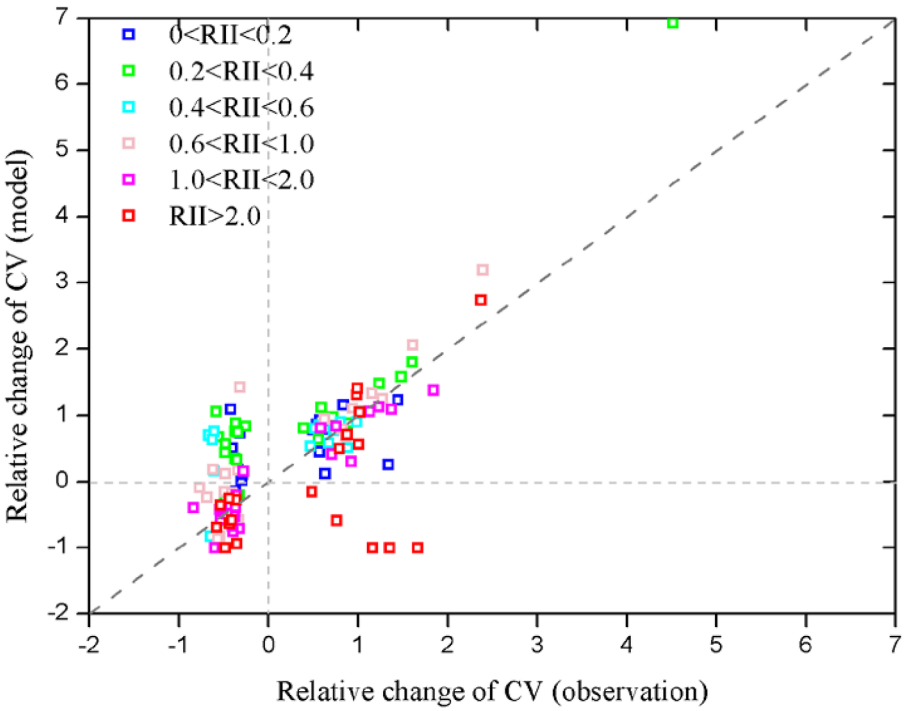

Figure 8. SOP2-simulated and observed relative change of the flood coefficient of variation (CV) for 123 gauges with their Reservoir Impact Index (RII) for six RII intervals shown in colors.

indicating that the reservoirs very likely have enough storage capacity to regulate most of the floods. For these basins, one possible explanation for the contradicting behavior is that other factors, such as irrigation and/or changing climate conditions, may dominate over the reservoir regulation effects, leading to the increased CV during the post-dam period.

The threshold behavior in the $\Delta MAF \sim RII$ relationship (namely how ΔMAF changes with RII) is consistently revealed by both the observed data (Figure 5) and the models (Figures 6 and 7). It is clear that the threshold behavior is mainly due to the flood-regulation process by the reservoirs so even a simple model such as SLM can capture the salient features of the observed behavior. Although the existence of threshold behavior in the $\Delta CV \sim RII$ relationship is suggested by all three models, it is not so obvious from the observed data so more investigation is warranted.

Figure 9 shows the $\Delta CV \sim RII$ relationship simulated by SOP2 at four selected gauges with relatively large (Gauge A and B) and small (Gauge C and D) RII values. The gauge information is listed in Table 2. The curves show how ΔCV varies as a function of regulation capacities. The dots indicate the actual reservoir regulation capacity values in the river systems and the corresponding observed ΔCV values. Figure 9 suggests that, for a specific river system, there is a theoretical value of RII around which the response of the river system to reservoir regulation can be divided into two regimes—a gradual increase of ΔCV with RII and a rapid drop of ΔCV with RII. However, the actual RII value of a real-world reservoir system could be located on either side of the theoretical RII threshold value, so the observed ΔCV values could be either positive or negative. Therefore, the post-dam CV at gauges with similar RII values (e.g., the red and black dots with larger RII values and the blue and green dots with small RII values) could change in different directions from the pre-dam values as shown in Figure 9. Figure 9 and its interpretations can be used to at least partly explain the observed symmetric change in ΔCV with RII (i.e., both positive and negative ΔCV values at the same RII as shown in Figure 5b).

The theoretical RII threshold value for a river system could be affected by uncertainties in the reservoir model parameters. So far a relatively uniform set of reservoir parameters, including Q_s, Q_d, S_n, and S_c have been used across the gauges to facilitate the modeling analysis. Figure 10 illustrates the impacts of reservoir

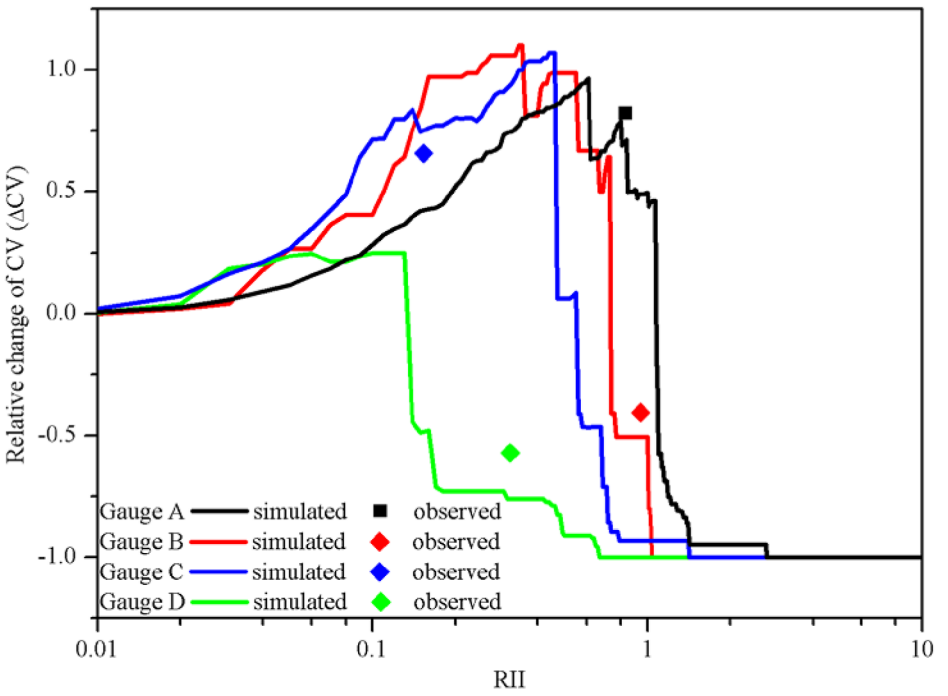

Figure 9. Comparison of the relative change in the flood coefficient of variation (ΔCV) as a function of Reservoir Impact Index (RII) simulated by the SOP2 model (colored lines) with observations (colored dots) at four gauges indicated by colors.

parameter uncertainty on the theoretical RII threshold value. According to the figure, Q_s is the most sensitive parameter that will impact the model results. The maximum safe discharge for the downstream area, Q_s, is a reservoir operation parameter that is usually subject to changes across space and time. A higher Q_s implies faster depletion of reservoir space and larger regulation capacity given the same storage capacity, hence leading to the left-shift of the RII threshold value. S_n only has a small effect on the result for obvious reasons. Before the flood season begins, the water level in the reservoir will decrease to S_c, no matter how big S_n is, as this is during the nonflood season. S_c will more strongly affects the floods, because lower S_c means more capacity to hold floods in the flood season. The effect of Q_d is similar to that of S_c. A higher Q_d means more water is released during the year, so more space is available to hold possible floods.

The theoretical RII threshold value could also depend on other factors. For example, the temporal variability of monthly streamflow and annual maximum flood peaks (e.g., inter and intra-annual variability) will affect the temporal variability of reservoir storage, and hence the regulation capacity. The existence of other peak flows that are smaller than the annual flood peaks but much larger than other daily flows (hence also regulated) could also affect the theoretical RII threshold value. A comprehensive investigation of all these controlling factors is left for future research.

Table 2
Gauge Information for Four Selected Gauges Used in the Data Analysis (MAF Stands for Mean Annual Floods, and AMS Stands for Annul Mean Streamflow)

Gauge	USGS ID	Name of gauge and stream	RII	Number of dams	MAF/AMS
Gauge A	01377000	Hackensack River at Rivervale, NJ	0.833	6	7.534
Gauge B	02060500	Roanoke River at Altavista, VA	0.944	37	18.025
Gauge C	02025500	James River at Holcomb Rock, VA	0.155	39	12.827
Gauge D	06790500	North Loup River near Saint Paul, Nebr.	0.315	36	5.064

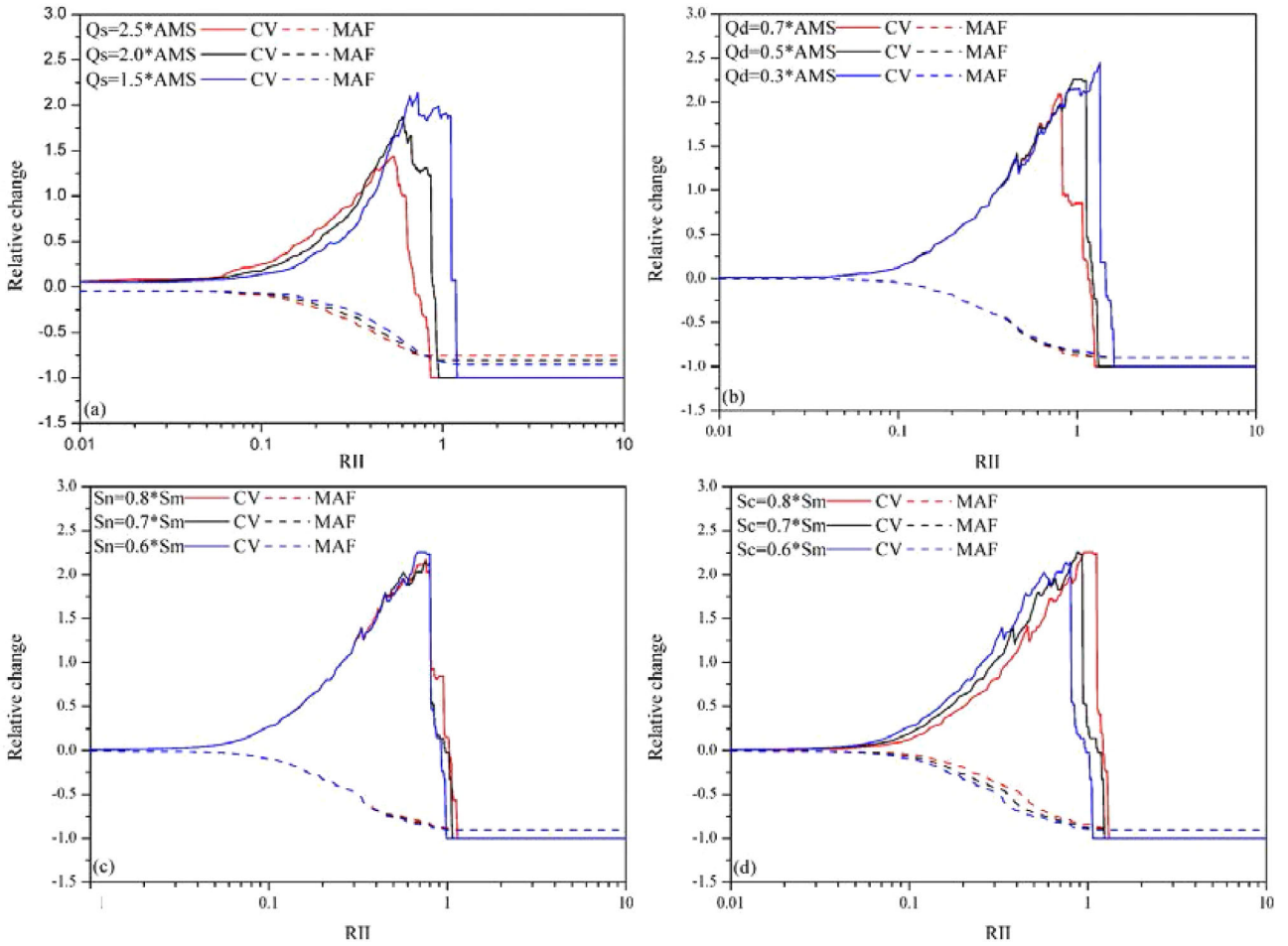

Figure 10. Impacts of reservoir parameter uncertainties related to (a) inflow threshold Qs; (b) water demand Qd; (c) normal storage Sn; and (d) flood limited storage Sc on the simulated relative changes in the maximum annual flood (MAF, dashed lines) and the coefficient of variation (CV, solid lines) simulated by the SOP2 model. In each plot, simulations for three perturbed parameter values are shown by different colors.

4. Discussion and Conclusions

This paper presents a combined data-modeling analysis of the nonlinear filtering effects of reservoir on the flood frequency curves (FFCs) across the United States. Two moments of the FFCs have been investigated: the mean annual flood (MAF) and the coefficient of variation (CV). Using a dimensionless Reservoir Impact Index (RII) to quantify the relative regulation capacity, a nonlinear threshold behavior has been revealed in the post-dam changes of both the MAF and CV from observations. Reservoir regulation is found to significantly modulate flooding but the filtering effects have a strong dependence on the relative regulation capacity. It is found that MAF generally decreases with increasing RII but stabilizes when RII exceeds a threshold value. CV increases with RII but decreases with RII beyond that threshold. Three simple but physically based reservoir models are used to investigate the role of the interactions between the reservoir and river systems. All models reproduce the threshold behavior of the $\Delta MAF \sim RII$ and $\Delta CV \sim RII$ relationships. Through the modeling analysis, we find that, when RII is small, the reservoir regulation has little effect on extremely large floods. This will enlarge the difference between large floods and small floods, which will result in the increase of CV. When RII is high enough, the reservoir will regulate all the floods and CV will decrease. The finding that even the simplest model (SLM) can capture the threshold behavior suggests that the basic flood control function of reservoirs is key to the nonlinear relationships, and reservoir can only mitigate floods within its capacity. However, the threshold RII values in the nonlinear $\Delta MAF \sim RII$ and $\Delta CV \sim RII$ relationships are dependent on the more detailed reservoir operations (e.g., initial storage) and objectives (e.g., water supply besides flood control) that are only captured by SOP1 and SOP2.

This paper advances a conceptual model of how reservoirs may affect FFCs, and through observation data we validate the effectiveness of the conceptual model on predicting changes in MAF and CV after regulation. It represents an extension to the work of Blöschl and Sivapalan (1997) which explored how natural factors control flood CV. They found that nonlinear runoff processes would increase flood CV. Compared with the natural routing process, reservoir regulation increases the nonlinearity of the runoff routing process when RII is relatively small. Consequently, reservoir regulation increases the flood CV in basins with small RII values. However, when RII is high enough, the regulated discharge will be more uniform, and the runoff routing process will be less nonlinear, resulting in a decrease of flood CV. From this perspective, our results remain consistent with Blöschl and Sivapalan (1997). Previous studies found that flood CV can be either decreased (Batalla et al., 2004) or increased (Assani et al., 2006) after reservoir regulation. Batalla et al. (2004) used an impounded runoff index similar to RII and found that flood variation was reduced after reservoir regulation at gauges with higher index. Assani et al. (2006) reported a notable increase in flood interannual variability for regulated watersheds larger than 10,000 km^2. However, none of the previous studies explains why reservoir operation influences flood CV differently. This paper provides an explanation of the mechanism behind this phenomenon using three physically based reservoir regulation models with different levels of complexity. Moreover, this study establishes a simple framework combining data analysis with modeling to explore the impacts of reservoir regulation on flood characteristics. Building on the current framework, it should be rather straightforward to couple SOP2 with hydrological models to predict future flood under the joint influences of climate change and reservoir regulation, or to apply SOP2 with derived flood frequency methodology (Sivapalan et al., 2005) to explore the cumulative impacts of climate change, land use, and reservoir regulation on flood.

Although the conceptual models are able to provide process understanding of the threshold behavior, some limitations of this study should be noted. First, except for SOP2, the simple models consider flood control as the only objective of the reservoirs so other functions such as irrigation, recreation, hydroelectricity, and fisheries are ignored. Therefore, our models mainly capture the behavior of flood control reservoirs but the FFC and CV changes are more complex for multipurpose reservoirs. Second, the interactions between reservoirs in a river system are not quantitatively incorporated. For example, the relative spatial locations among the reservoirs and between the reservoirs and the river gauges are not considered. This exclusion disregards the possible conjunctive operation of cascading reservoirs and any lateral inflow between the two reservoir locations, which can potentially affect the shape of the FFC curve. A more comprehensive RII can be defined by using the ratio of discharge at the dam location and the discharge at the gauge as a weight, as modified from the method of Brown and Carriquiry (2007), which uses drainage area as a weight. Such an improvement of RII should be more physical and reasonable. As the purpose of this paper is an assessment of the first-order reservoir effects at the regional scale, these simplifications are deemed appropriate. Further improvement of SOP2 and the RII definition is left for our future work.

While this paper studies the impact of reservoir regulation on the FFC, land use, and climate change could also have significant impacts on runoff generation and routing processes and subsequently on the FFCs (Hall et al., 2014; Viglione et al., 2016). Despite our selection of stream gauges to exclude the gauges subject to significant changes in annual mean streamflow caused by land use and climate changes, these may influence streamflow seasonality, which may also have impact on floods. Last but not least, RII is defined based on annual mean streamflow only, without accounting for the inter and intra-annual variability of flood peaks. Future research may pursue a more comprehensive definition of RII.

Notwithstanding the simplifications of the modeling study motivated by the regional-scale focus, the conclusions of this study have important implications in a number of areas. First, effects of the reservoir characteristics on the FFC may provide guidance in regional-scale planning of hydraulic structures in complex river systems, in particular if the region contains a large number of reservoirs. Second, the results may be useful for more robust flood frequency analysis in regulated river systems. If the FFC is reshaped by the reservoirs, the basic assumption of stationarity no longer holds. Pre-dam and post-dam records should be separately analyzed to transform the pre-dam floods to regulated floods so that combining them with the post-dam floods, a new stable and stationary flood series can be derived for the design of new hydraulic structures downstream of existing reservoirs. All of these will help improve flood-risk assessment and mitigation in large, regulated river systems.

Acknowledgments
This research was supported by the Office of Science of the US Department of Energy Biological and Environmental Research as part of the Integrated Assessment Research Program and Regional and Global Climate Modeling Program. PNNL is operated for DOE by Battelle Memorial Institute under contract DE-AC05–76RL01830. Wei Wang and Hui Lu were also supported by the National Basic Research Program of China (2015CB953703) and National Natural Science Foundation of China (91537210 and 41371328). Günter Blöschl would like to acknowledge the support from the Austrian Science Funds FWF (Doctoral Programme on Water Resource Systems DK-plus W1219-N22 and project P 23723-N21), and the ERC Flood Change Project (ERC advanced grant, 291152). All the data and scripts used in this study are available upon request.

References

Archfield, S. A., Hirsch, R. M., Viglione, A., & Blöschl, G. (2016). Change across the United States. *Geophysical Research Letters*, *43*, 10232–10239. https://doi.org/10.1002/2016GL070590

Assani, A. A., Stichelbout, E., Roy, A. E. G., & Petit, F. C. C. O. (2006). Comparison of impacts of dams on the annual maximum flow characteristics in three regulated hydrologic regimes in Québec (Canada). *Hydrological Processes*, *20*(16), 3485–3501.

Batalla, R. J., Gomez, C. M., & Kondolf, G. M. (2004). Reservoir-induced hydrological changes in the Ebro River basin (NE Spain). *Journal of Hydrology*, *290*(1), 117–136.

Blöschl, G., & Sivapalan, M. (1997). Process controls on regional flood frequency: Coefficient of variation and basin scale. *Water Resources Research*, *33*(12), 2967–2980.

Brown, C., & Carriquiry, M. (2007). Managing hydroclimatological risk to water supply with option contracts and reservoir index insurance. *Water Resources Research*, *43*, W11423. https://doi.org/10.1029/2007WR006093

Edward Miller, G. (1991). Use of the squared ranks test to test for the equality of the coefficients of variation. *Communication in Statics Simulation and Computation*, *20*(2–3), 743–750.

Falcone, J. A. (2011). GAGES-II: Geospatial attributes of gages for evaluating streamflow (Digital spatial data set). Retrieved from http://water.usgs.gov/GIS/metadata/usgswrd/XML/gagesII_Sept2011.xml (last accessed 10 October 2013).

Franks, S. W., & Kuczera, G. (2002). Flood frequency analysis: Evidence and implications of secular climate variability, New South Wales. *Water Resources Research*, *38*(5), 1062. https://doi.org/10.1029/2001WR000232

Gastwirth, J. L., Gel, Y. R., & Miao, W. (2009). The impact of Levene's test of equality of variances on statistical theory and practice. *Statistical Science*, *24*(3), 343–360.

Gilroy, K. L., & McCuen, R. H. (2009). Spatio-temporal effects of low impact development practices. *Journal of Hydrology*, *367*(3), 228–236.

Gilroy, K. L., & McCuen, R. H. (2012). A nonstationary flood frequency analysis method to adjust for future climate change and urbanization. *Journal of Hydrology*, *414*, 40–48.

Gringorten, I. I. (1963). A plotting rule for extreme probability paper. *Journal of Geophysical Research*, *68*(3), 813–814.

Guo, J., Li, H., Leung, L. R., Guo, S., Liu, P., & Sivapalan, M. (2014). Links between flood frequency and annual water balance behaviors: A basis for similarity and regionalization. *Water Resources Research*, *50*, 937–953.

Hall, J., Arheimer, B., Borga, M., Br A Zdil, R., Claps, P., Kiss, A., & Lang, M. (2014). Understanding flood regime changes in Europe: A state of the art assessment. *Hydrology and Earth System Science*, *18*, 2735–2772.

Khaliq, M. N., Ouarda, T., Ondo, J., Gachon, P., & Bobée, B. (2006). Frequency analysis of a sequence of dependent and/or non-stationary hydro-meteorological observations: A review. *Journal of Hydrology*, *329*(3), 534–552.

Lehner, B., Liermann, C. R., Revenga, C., Voro Smarty, C., Fekete, B., Crouzet, P., . . . Magome, J. (2011). *Global reservoir and dam (GRanD) database. Version 1.1*. Bonn, Germany: Global Water System Project.

Leung, L. R., Qian, Y., Bian, X., Washington, W. M., Han, J., & Roads, J. O. (2004). Mid-century ensemble regional climate change scenarios for the western United States. *Climatic Change*, *62*(1), 75–113.

López, J., & Francés, F. (2013). Non-stationary flood frequency analysis in continental Spanish rivers, using climate and reservoir indices as external covariates. *Hydrology and Earth System Science*, *17*, 3189–3203.

Magilligan, F. J., & Nislow, K. H. (2005). Changes in hydrologic regime by dams. *Geomorphology*, *71*(1), 61–78.

Maheshwari, B. L., Walker, K. F., & McMahon, T. A. (1995). Effects of regulation on the flow regime of the River Murray, Australia. *Regulated Rivers: Research\& Management*, *10*(1), 15–38.

Mallakpour, I., & Villarini, G. (2015). The changing nature of flooding across the central United States. *Nature Climate Change*, *5*(3), 250–254.

Mann, H. B., & Whitney, D. R. (1947). On a test of whether one of two random variables is stochastically larger than the other. *The Annals of Mathematical Statistics*, *18*(1), 50–60.

Merz, B., Vorogushyn, S., Uhlemann, S., Delgado, J., & Hundecha, Y. (2012). HESS Opinions'' more efforts and scientific rigour are needed to attribute trends in flood time series''. *Hydrology and Earth System Science*, *16*(5), 1379–1387.

Messner, F., & Meyer, V. (2006). Flood damage, vulnerability and risk perception–challenges for flood damage research. In J. Schanze, E. Zeman & J. Marsalek (Eds.), *Flood risk management: Hazards, vulnerability and mitigation measures* (pp. 149–167). Ostrov, Czech Republic: Springer.

Milly, P. (2007), Stationarity is dead, *Ground Water News & Views*, *4*(1), 6–8.

Morris, G. L., & Fan, J. (1998). *Reservoir sedimentation handbook: Design and management of dams, reservoirs, and watersheds for sustainable use*. New York, NY: McGraw-Hill.

Niehoff, D., Fritsch, U., & Bronstert, A. (2002). Land-use impacts on storm-runoff generation: Scenarios of land-use change and simulation of hydrological response in a meso-scale catchment in SW-Germany. *Journal of Hydrology*, *267*, 80–93.

Robinson, J. S., & Sivapalan, M. (1997). An investigation into the physical causes of scaling and heterogeneity of regional flood frequency. *Water Resources Research*, *33*(5), 1045–1059.

Rosbjerg, D., Bloschl, G., Burn, D. H., Castellarin, A., Croke, B., Baldassarre, G. D.,. . . Viglione, A. (2013). Prediction of floods in ungauged basins. In G. Bloschl (Ed.), *Runoff prediction in ungauged basins: Synthesis across processes, places and scales* (pp. 189–226). Cambridge, UK: Cambridge Univ. Press.

Sivapalan, M., Blöschl G., Merz, R., & Gutknecht, D. (2005). Linking flood frequency to long-term water balance: Incorporating effects of seasonality. *Water Resources Research*, *41*, W06012. https://doi.org/10.1029/2004WR003439

Sivapalan, M., Wood, E. F., & Beven, K. J. (1990). On hydrologic similarity: 3. A dimensionless flood frequency model using a generalized geomorphologic unit hydrograph and partial area runoff generation. *Water Resources Research*, *26*(1), 43–58.

Tennant, D. L. (1976), Instream flow regimens for fish, wildlife, recreation and related environmental resources. *FISHERIES*, *1*(4), 6–10.

Trenberth, K. E. (2011). Changes in precipitation with climate change. *Climate Research*, *47*(1), 123–138.

Viglione, A., Merz, B., Viet Dung, N., Parajka, J., Nester, T., & Blöschl, G. (2016). Attribution of regional flood changes based on scaling fingerprints. *Water Resources Research*, *52*, 5322–5340. https://doi.org/10.1002/2016WR019036

Villarini, G., Serinaldi, F., Smith, J. A., & Krajewski, W. F. (2009). On the stationarity of annual flood peaks in the continental United States during the 20th century. *Water Resources Research*, *45*, W08417. https://doi.org/10.1029/2008WR007645

Vogel, R. M., & Wilson, I. (1996). Probability distribution of annual maximum, mean, and minimum stream flows in the United States. *Journal of Hydrologic Engineering*, *1*(2), 69–76.

Wright, D. B., Smith, J. A., & Baeck, M. L. (2014). Flood frequency analysis using radar rainfall fields and stochastic storm transposition. *Water Resources Research*, *50*, 1592–1615.

Yang, L., Smith, J. A., Wright, D. B., Baeck, M. L., Villarini, G., Tian, F., & Hu, H. (2013). Urbanization and climate change: An examination of nonstationarities in urban flooding. *Journal of Hydrometeorology*, *14*(6), 1791–1809.